# Plasmon-soliton waves in planar slot waveguides. I. Modeling

Wiktor Walasik[1,2] and Gilles Renversez[1,*]

[1]*Aix–Marseille Université, CNRS, Centrale Marseille, Institut Fresnel, UMR 7249, 13013 Marseille, France*

[2]*ICFO — Institut de Ciències Fotòniques, Universitat Politècnica de Catalunya, 08860 Castelldefels (Barcelona), Spain*

(Received 30 June 2015; revised manuscript received 17 September 2015; published 14 January 2016)

We present two complementary models to study stationary nonlinear solutions in one-dimensional plasmonic slot waveguides made of a finite-thickness nonlinear dielectric core surrounded by metal regions. The considered nonlinearity is of focusing Kerr type. In the first model, it is assumed that the nonlinear term depends only on the transverse component of the electric field and that the nonlinear refractive index change is small compared to the linear part of the refractive index. This first model allows us to describe analytically the field profiles in the whole waveguide using Jacobi elliptic special functions. It also provides a closed analytical formula for the nonlinear dispersion relation. In the second model, the full dependency of the Kerr nonlinearity on the electric-field components is taken into account and no assumption is required on the amplitude of the nonlinear term. The disadvantage of this approach is that the field profiles must be computed numerically. Nevertheless, analytical constraints are obtained to reduce the parameter space where the solutions of the nonlinear dispersion relations are sought.

DOI: 10.1103/PhysRevA.93.013825

## I. INTRODUCTION

Studies of stationary nonlinear waves possessing the properties of both plasmons and solitons started in the early 1980s when this type of waves was described by Agranovich *et al.* [1]. Two main types of structures supporting plasmon-soliton waves were studied. The first type contains one or two semi-infinite nonlinear media and was extensively studied in Refs. [2–16]. Transverse electric (TE) and transverse magnetic (TM) polarized waves were investigated in configurations built of semi-infinite nonlinear layers, a metal layer, and, in some cases, additional dielectric layers. The second type of structure contains a finite-size nonlinear dielectric layer sandwiched between two semi-infinite metal layers. This type of structure will be called here nonlinear slot waveguide (NSW). Studies of configurations with a nonlinear dielectric core started in the early 1980s from fully dielectric structures [17–23]. The solutions of Maxwell's equations in a finite-size nonlinear dielectric were given in terms of Jacobi elliptic functions [24]. A symmetry breaking bifurcation was predicted for the fundamental symmetric mode giving birth to an asymmetric mode [18,19]. Various methods to study fully dielectric waveguides with both nonlinear core and cladding were proposed [25–32].

In 2007, Feigenbaum and Orenstein [33] made the first attempt to study waveguides with a nonlinear core surrounded by a metal cladding (NSWs) instead of a dielectric one. Their method describes subwavelength confinement of light in two-dimensional plasmon-soliton beams propagating in NSWs. Such a strong confinement is ensured by a linear plasmon profile in the transverse direction and by the self-focusing effect in the lateral direction. Recently, numerical [34] and semianalytical [35,36] methods have been developed to study up to the three first nonlinear modes in NSWs. Higher-order modes were also reported in NSWs [37].

The NSW is an interesting and promising configuration for two reasons: (i) from the practical point of view, it is easier to fabricate high quality thin nonlinear films than bulky layers, like those needed in the configurations with semi-infinite nonlinear medium and (ii) it has numerous potential applications. Devices based on the NSW configuration can be used for phase matching in higher-harmonic generation processes [38] and for nonlinear plasmonic couplers [39,40]. Nonlinear switching [41] was theoretically predicted in NSW-based structures that is similar to the nonlinear switching in graphene couplers [42]. Tapered NSWs might be used for nanofocusing and loss compensation in order to enhance nonlinear effects [43].

The field of NSWs is relatively young and there is not a lot of work describing the properties of these structures. In this article, we build two new and complementary models that allow us to study efficiently and accurately the NSW configurations. These models have been briefly and partially introduced in Ref. [37] and here we present their detailed derivations.

In Sec. II, a general description of the problem studied here is given. Section III presents the theoretical derivation of our two models. These models are used to thoroughly study the propagation of plasmon-soliton waves in NSWs in the following article [44], where analytical and numerical stability analysis results are also provided.

## II. PROBLEM STATEMENT

This article presents a derivation of the dispersion relations for the stationary TM polarized waves propagating in one-dimensional NSWs depicted schematically in Fig. 1. We propose two models to study the light propagation in such structures. The first model is based on the approach proposed for fully dielectric structures in [17,20] extending it to structures containing metals. Due to the presence of the metal cladding, the field continuity conditions result in a new type of field profiles and very rich dispersion relations. This approach uses an approximated treatment of the nonlinearity

*gilles.renversez@univ-amu.fr

 

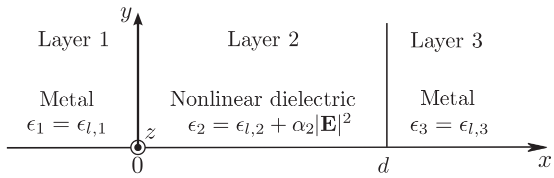


FIG. 1. Geometry of the plasmonic NSW with the parameters of the structure.

in the Kerr medium which allows us to write and solve a single nonlinear wave equation in the finite-size nonlinear medium. Using the field continuity conditions at the core interfaces located at $x = 0$ and $x = d$, the analytical formulas for the dispersion relations and for the field profiles are obtained in terms of Jacobi elliptic functions [24]. Therefore, this model will be called Jacobi elliptic function based model (JEM).

The first step of our second model is based on the approaches from Refs. [9,10] for a single interface between a nonlinear dielectric and a metal. The second step of this model is a new extension to treat the two-interface case of the finite-size nonlinear region. It will be named the interface model (IM). This model uses a more realistic treatment of the nonlinear Kerr effect than the JEM (i.e., Kerr nonlinearity depends on all the components of the electric field). It allows us to obtain separate dispersion relations on the two interfaces of the NSW in analytical forms. Comparing the dispersion equations for the left interface and for the right interface results in an analytical condition that reduces the parameter space in which the solutions of Maxwell's equations in NSWs are sought. The solutions are found by the numerical integration of Maxwell's equation in the core which allows one to relate the two interfaces. Maxwell's equations in the core are solved using the shooting method [45]. If the result of integration is consistent with the previously assumed values of the field and its derivatives at the slot interfaces, then the corresponding effective index $\beta$ is accepted as a genuine solution in our problem.

The stationary solutions in our one-dimensional geometry are sought in the form of monochromatic harmonic waves:

$$\begin{Bmatrix} \mathscr{E}(x,z,t) \\ \mathscr{H}(x,z,t) \end{Bmatrix} = \begin{Bmatrix} \mathbf{E}(x) \\ \mathbf{H}(x) \end{Bmatrix} e^{i(k_0\beta z - \omega t)}, \tag{1}$$

where $\mathbf{E} = [E_x, 0, iE_z]$ and $\mathbf{H} = [0, H_y, 0]$. We write the imaginary unit $i$ in front of the $z$ component of the electric field so that all the quantities $E_x$, $E_z$, and $H_y$ are real. The propagation direction is chosen to be $z$ and $\omega$ denotes the angular frequency of the wave. $k_0 = \omega/c$ denotes the wave number in vacuum, and $c$ denotes the speed of light in vacuum. The effective index of the wave is defined as $\beta$, so that the propagation constant is given by $k_0\beta$. The structure is invariant along the $y$ direction and, therefore, it is assumed that the field profiles are invariant along the $y$ coordinate.

## III. MODEL DERIVATION

### A. Maxwell's equations

The derivation of our models starts from the general form of Maxwell's equations in the case of nonmagnetic materials (relative permeability $\mu = 1$) without free charges ($\rho_f = 0$) and free currents ($\mathbf{J}_f = 0$) [46]. For the harmonic monochromatic TM waves described by Eq. (1) and for an isotropic relative permittivity $\epsilon$ the Maxwell's equations read

$$k_0\beta E_x - \frac{dE_z}{dx} = \omega\mu_0 H_y, \tag{2a}$$

$$E_x = \frac{\beta}{\epsilon_0\epsilon c} H_y, \tag{2b}$$

$$E_z = \frac{1}{\epsilon_0\epsilon\omega}\frac{dH_y}{dx}, \tag{2c}$$

where $\epsilon_0$ and $\mu_0$ denote vacuum permittivity and permeability, respectively. The nonlinearity studied here is of the Kerr type

$$\epsilon = \epsilon_l(x) + \epsilon_{\rm nl}(x), \tag{3}$$

where $\epsilon_l$ denotes the linear, real part of the permittivity, $\epsilon_{\rm nl} = \alpha(x)|\mathbf{E}(x)|^2$ describes the nonlinear part of the permittivity limited to the isotropic optical Kerr effect that depends on the electric field intensity, and $\alpha(x)$ is the function that takes values of the nonlinear parameters associated with different layers (in linear materials it is null). The imaginary part of the permittivity is neglected in the modal studies presented here.

The formulation of the Kerr effect used in this study can be found in the majority of the works on the nonlinear waveguides and nonlinear surface waves [1–7,9–23,25–30,33–36,47–74]. It describes sufficiently well the nonlinear effects studied here. As a first approximation, to describe the physics of our system we do not need to use the more complex form of the Kerr nonlinear term which was described in Ref. [75].

### B. Jacobi elliptic function based model

We start the presentation of the models for NSWs with the approach that uses strong assumptions on the form of the nonlinear Kerr term but it provides the dispersion relations and the field profiles in analytical forms. This model provides more insight and understanding of the nature of the problem of finding stationary solutions in NSWs than the second, more numerical model. First, we will solve the nonlinear wave equation inside the waveguide core and find the nonlinear field profiles. Knowing the field profiles, we will be able to derive the dispersion relations for the NSW using the continuity conditions on the two nonlinear core interfaces.

#### *1. Assumptions*

In the frame of the Jacobi elliptic function based model (JEM), the Kerr-type nonlinearity is not treated in an exact manner. We assume that the nonlinear response of the material is isotropic and depends only on the transverse component of the electric field $E_x$ in the following way [12,16,37]:

$$\epsilon(x) = \epsilon_l(x) + \alpha(x)E_x^2(x). \tag{4}$$

Functions $\epsilon_l(x)$ and $\alpha(x)$ are stepwise functions which take the values indicated in Table I depending on the layer (see Fig. 1 for layer numbering).

TABLE I. Values of the functions $\epsilon_l(x)$ and $\alpha(x)$ describing the properties of the materials in different layers. The nonlinear parameter $n_2$ in layer 2 is denoted by $n_2^{(2)}$.

| Layer | Abscissa | $\epsilon_l(x)$ | $\alpha(x)$ |
|---|---|---|---|
| 1 | $x < 0$ | $\epsilon_1 = \epsilon_{l,1}$ | 0 |
| 2 | $0 \leqslant x \leqslant d$ | $\epsilon_{l,2}$ | $\epsilon_0 c \epsilon_{l,2} n_2^{(2)} = \alpha_2$ |
| 3 | $x > d$ | $\epsilon_3 = \epsilon_{l,3}$ | 0 |

#### *2. Derivation of the nonlinear dispersion equation*

The derivation of the JEM starts with Eqs. (2). These equations are combined together with Eq. (4) and, with the help of the approximations about small nonlinear permittivity change, we obtain the nonlinear wave equation:

$$\frac{d^2 H_y}{dx^2} - k_0^2 q^2(x) H_y + k_0^2 a(x) H_y^3 = 0, \tag{5}$$

where

$$q^2(x) = \beta^2 - \epsilon_l(x), \quad a(x) = \beta^2 \alpha(x)/[\epsilon_0 \epsilon_l(x) c]^2, \tag{6}$$

and we have used the relations $\omega = c k_0$ and $c^2 = 1/(\epsilon_0 \mu_0)$. For the $q$ notation used in Eq. (6), we follow the definition already used in several articles including ones dedicated to the slot configuration that allows a general definition valid for all the structure layers even if in the nonlinear core, for some cases, $q^2(x)$ can be negative [1,4,6,16,38]. A detailed derivation of Eq. (5) is presented in Refs. [16,76]. We use the first-integral treatment approach [9,10] and integrate Eq. (5) in each of the structure layers separately. The result reads

$$\left(\frac{dH_y}{dx}\right)^2 - k_0^2 q(x)^2 H_y^2 + k_0^2 \frac{a(x)}{2} H_y^4 = c_0(x). \tag{7}$$

The right-hand side of this equation is given by a piecewise function $c_0(x)$ that corresponds to the value of the integration constant in each layer. The left-hand side of Eq. (7) gives us a formula for a field based quantity that is constant in each of the layers of our one-dimensional nonlinear waveguide. In semi-infinite layers (layers 1 and 3) [16], the function $c_0(x)$ is zero, because both the magnetic field $H_y$ and its derivative $dH_y/dx$ tend to zero as $x \to \pm\infty$. Additionally, in these linear layers $a(x)$ is equal to zero. Thus, in the cladding, Eqs. (5) reduces to a standard linear wave equation whose solutions are given by

$$H_1 = H_0 e^{k_0 q_1 x} \quad \text{for} -\infty \leqslant x < 0, \tag{8a}$$

$$H_3 = H_d e^{-k_0 q_3 (x-d)} \quad \text{for } d \leqslant x < +\infty, \tag{8b}$$

where only the appropriate exponential solutions are considered. Here the magnetic-field amplitudes at the interfaces $x = 0$ and $x = d$ are denoted by $H_0$ and $H_d$, respectively, and $q_k$ denotes a constant value of the $q(x)$ function in $k$th layer (for $k \in \{1,2,3\}$) since $\epsilon_l(x)$ is piecewise constant. In the nonlinear core of our structure, the function $c_0(x)$ takes a constant value denoted hereafter as $c_0$. Inside of this core region regardless of at which $x$ abscissa we calculate the left-hand side of Eq. (7), the result will always be equal to the integration constant $c_0$.

Since $H_y$ is the only component of the magnetic field, in the following derivation we omit the $y$ subscript and instead we use a subscript that enumerates the layer in which the field profile is defined (see Fig. 1). It is worth mentioning that this derivation is fully different from the one described in Ref. [16] due to the fact that, in the present study, the size of the nonlinear region is finite and not semi-infinite which precludes the use of the well-known secant hyperbolic function and forces the use of Jacobi elliptic functions and a careful analysis of the continuity conditions at the core interfaces.

The integration constant $c_0$ can be expressed as a function of the magnetic-field amplitude $H_0$ using the continuity conditions for the tangential electromagnetic-field components $(H_y, E_z)$ at $x = 0$ in Eq. (7):

$$c_0 = k_0^2 \left[ (\epsilon_{l,2}/\epsilon_1)^2 q_1^2 - q_2^2 + a_2 H_0^2/2 \right] H_0^2, \tag{9}$$

where $a_2$ denotes the constant value of $a(x)$ function in the nonlinear core [layer 2; see Eq. (6) and Table I] and where, based on the assumption that the nonlinear permittivity change is small, we have substituted $\epsilon_2|_{x=0^+}$ by $\epsilon_{l,2}$ in the fraction numerator. Similar expression can be obtained for the second interface at $x = d$. Equations (7) and (9) allow us to find the sign of the integration constant $c_0$ for certain types of solutions. The solutions can be later classified according to the sign of $c_0$. Looking at Eq. (7) we notice that for $H_y$ field profiles that cross zero, at the point where $H_y = 0$, the only nonzero term on the left-hand side of this equation is $(dH_y/dx)^2$, which is strictly positive. Therefore, for this type of solution, $c_0$ can only be positive. From Eq. (9) we notice that for negative $q_2^2$, the value of the integration constant $c_0$ is also positive.

We are searching for guided waves in three-layer structures. Looking at Eqs. (8), we notice that the condition for the waves to be localized in the waveguide core is satisfied when both $q_1$ and $q_3$ are real and positive quantities. In order to satisfy this condition, we will look only for the solutions with $\beta^2 > \max\{\epsilon_1, \epsilon_3\}$ [for the definition of $q(x)$ and $q_k$; see Eq. (6) and the text after Eqs. (8)]. The quantity $q_2$ can be either real or imaginary leading to positive or negative values of $q_2^2$.

In order to find the solutions of the nonlinear wave equation [Eq. (5)] in the nonlinear core, we rewrite its first integral [Eq. (7)] in the form

$$\frac{dH_2}{\sqrt{Ac_0 + AQH_2^2 - H_2^4}} = \pm\sqrt{\frac{1}{A}} dx, \tag{10}$$

using the reduced parameters $Q$ and $A$:

$$Q = k_0^2 q_2^2, \quad A = \left(k_0^2 a_2/2\right)^{-1}. \tag{11}$$

In this study, we deal only with the focusing Kerr-type dielectrics; therefore, $A$ is always positive. Parameter $Q$ can be either positive or negative depending on the sign of $q_2^2$. Solutions of Eq. (10) take different forms depending on the sign of parameter $c_0$. We will solve this equation in the two possible cases. The detail of this derivation is provided in Ref. [76].

*First case:* $c_0 > 0$. At first, we consider the case where $c_0 > 0$. The solution of the nonlinear wave equation [Eq. (7) or Eq. (10)] for this case is given by

$$H_2(x) = \delta \, \text{cn}\{\sqrt{s/A}\,(x - x_0)|m\}, \tag{12}$$

where $\mathrm{cn}(u|m)$ is a Jacobi elliptic function with an argument $u$ and a parameter $m$ [24], and

$$m = \delta^2/s, \quad s = \gamma^2 + \delta^2, \tag{13a}$$

$$\gamma^2 = (\sqrt{A^2Q^2 + 4Ac_0} - AQ)/2, \tag{13b}$$

$$\delta^2 = (\sqrt{A^2Q^2 + 4Ac_0} + AQ)/2, \tag{13c}$$

$$x_0 = -\sqrt{A/s}\,\mathrm{cn}^{-1}\left[H_2(0)/\delta|m\right]. \tag{13d}$$

Here $\mathrm{cn}^{-1}(u|m)$ is the inverse of the Jacobi elliptic function $\mathrm{cn}(u|m)$.

Now we derive the dispersion relation for NSWs. Using the analytical formula for the field profile in the nonlinear core [Eq. (12)], the field profiles in metal claddings given by Eqs. (8), and Maxwell's equations [Eqs. (2)], we write the continuity conditions for the tangential electromagnetic-field components $H_y$ and $E_z$ at the interfaces between the nonlinear core and the metal cladding $x = d$ (the continuity conditions at $x = 0$ was already used to evaluate the integration constant [see Eq. (9)]) as follows.

(1) The continuity condition for the magnetic-field component $H_2|_{x=d^-} = H_3|_{x=d^+}$ yields

$$\delta\ \mathrm{cn}[\sqrt{s/A}\ (d - x_0)\ |\ m] = H_d. \tag{14}$$

(2) The continuity condition for the tangential electric-field component $E_{z,2}|_{x=d^-} = E_{z,3}|_{x=d^+}$ transformed with the use of Eq. (2c), the formulas for the Jacobi elliptic function derivatives, and the symmetry properties of Jacobi elliptic functions gives

$$\delta\epsilon_3\sqrt{s}/(k_0q_3\epsilon_{l,2}\sqrt{A})\,\mathrm{sn}[\sqrt{s/A}\ (d - x_0)\ |\ m] \times \mathrm{dn}[\sqrt{s/A}\ (d - x_0)|m] = H_d, \tag{15}$$

where, based on the assumption that the nonlinear permittivity change is small, we substituted $\epsilon_2|_{x=0^+}$ by $\epsilon_{l,2}$ in the denominator on the left-hand side.

Comparing the two expressions for $H_d$ given by Eqs. (14) and (15), we obtain the nonlinear dispersion relation in its final form for the case of $c_0 > 0$:

$$\begin{aligned} k_0q_3\epsilon_{l,2}\sqrt{A}\,\mathrm{cn}[\sqrt{s/A}(d - x_0)|m] \\ = \epsilon_3k_0q_3\epsilon_{l,2}\sqrt{s}\,\mathrm{sn}[\sqrt{s/A}\ (d - x_0)|m] \\ \times\ \mathrm{dn}[\sqrt{s/A}\ (d - x_0)|m]. \end{aligned} \tag{16}$$

*Second case:* $c_0 < 0$. For $c_0 < 0$, the solution of the nonlinear wave equation [Eq. (7) or Eq. (10)] is given by

$$H_2(x) = \gamma\ \mathrm{dn}\{\sqrt{\gamma^2/A}\ (x - x_0)|m\}, \tag{17}$$

where $\mathrm{dn}(u|m)$ is a Jacobi elliptic function [24] and

$$m = (\gamma^2 - \delta^2)/\gamma^2, \tag{18a}$$

$$\gamma^2 = (AQ + \sqrt{A^2Q^2 - 4A|c_0|})/2, \tag{18b}$$

$$\delta^2 = (AQ - \sqrt{A^2Q^2 - 4A|c_0|})/2, \tag{18c}$$

$$x_0 = -\sqrt{A/\gamma^2}\,\mathrm{dn}^{-1}[H_2(0)/\gamma|m]. \tag{18d}$$

Here $\mathrm{dn}^{-1}(u|m)$ is the inverse of the Jacobi elliptic function $\mathrm{dn}(u|m)$.

The method used to derive the dispersion relation for this case is exactly the same as in the previous one. Using the analytical formula for the field profile in the nonlinear core [Eq. (17)], the field profiles in metal claddings given by Eqs. (8), and Maxwell's equations [Eqs. (2)], we write the continuity conditions for the tangential electromagnetic-field components $H_y$ and $E_z$ at the interfaces between the nonlinear core and the metal cladding $x = d$. The two resulting expressions for $H_d$ are compared and give the nonlinear dispersion relation in its final form for the case $c_0 < 0$:

$$\begin{aligned} k_0q_3\epsilon_{l,2}\sqrt{A}\,\mathrm{dn}[\sqrt{\gamma^2/A}(d - x_0)|m] \\ = \epsilon_3 m\sqrt{\gamma^2}\,\mathrm{sn}[\sqrt{\gamma^2/A}\ (d - x_0)|m] \\ \times\ \mathrm{cn}[\sqrt{\gamma^2/A}\ (d - x_0)|m]. \end{aligned} \tag{19}$$

Equations (16) and (19) build the full dispersion relation for the NSW. In order to obtain the dispersion diagram for a fixed structure and wavelength ($\epsilon_1$, $\epsilon_{l,2}$, $n_2^{(2)}$, $\epsilon_3$, $d$, $\lambda$) we scan $H_0$ values. For a fixed $H_0$, using Eq. (9) we identify intervals of $\beta$ where $c_0$ is positive or negative. In these intervals, we find $\beta$ values that satisfy Eq. (16) or Eq. (19) depending on the sign of $c_0$. The resulting nonlinear dispersion curves of the NSW are given in Figs. 1(a) and 7 of the following article [44].

### C. Interface model

In Sec. III B, we have derived the JEM that treats the Kerr nonlinearity present in the core of the NSW in a simplified way [see Eq. (4)]. The used assumptions allowed us to obtain analytical formulas for the nonlinear dispersion relations and the field profiles of the nonlinear modes of the NSW.

In this section, we will present the derivation of a model that is more numerical than the JEM but treats the Kerr-type nonlinearity in a more precise way. It is well known that the general expression of the nonlinear term involves the fourth-rank third-order susceptibility tensor [77] and all the electric-field components. In the simple case where the nonlinear medium is assumed to be isotropic, the full expression of the nonlinear term can be chosen as proportional to the squared norm of the electric field as it is often used in nonlinear waveguide studies [10,78]. In the present case (we are studying TM waves) the electric field has only two non null components $E_x$ and $E_z$, and as it will be shown later in the following article [44] $|E_z|$ is not always negligible compared to $|E_x|$ in the nonlinear slot waveguides with metal cladding. Consequently, the permittivity of the nonlinear core in the frame of the interface model (IM) is described by

$$\epsilon_2(x) = \epsilon_{l,2}(x) + \alpha_2\left[E_x^2(x) + E_z^2(x)\right]. \tag{20}$$

Moreover, there is no theoretical limitation of the values of the nonlinear permittivity change. In the IM, the solutions of Maxwell's equations are sought numerically, as explained in the following. The field profiles inside the nonlinear core are found by numerical integration of Maxwell's equations that couple the $E_x$ and $E_z$ field components. The novelty of our numerical method lays in the fact that the parameter space where the solutions are being sought is reduced by a constraint that is expressed in an analytical form. Below the derivation of this constraint is presented and the numerical procedure of finding the nonlinear dispersion relations using the IM is shortly described.

#### 1. Analytical constraint

The derivation of the IM starts from Maxwell's equations [Eqs. (2)]. In this approach the magnetic field is eliminated from these equations. The use of Eq. (2b) in Eqs. (2a) and (2c) gives [10,16,37,76]

$$\frac{dE_z}{dx} = k_0\left(\beta - \frac{\epsilon}{\beta}\right)E_x, \tag{21a}$$

$$\frac{d(\epsilon E_x)}{dx} = \beta k_0 \epsilon E_z. \tag{21b}$$

Let us first consider the region of the nonlinear core. In this region, Eq. (21a) is derived with respect to $x$, and transformed with the use of Eqs. (21b) and (20). Then, we use the first-integral approach, and integrate by parts the resulting equation, to finally obtain (for the detailed derivation see Ref. [76])

$$\left(\frac{dE_z}{dx}\right)^2 = (\beta k_0)^2 E_x^2 - k_0^2 \epsilon_{l,2}\left(E_x^2 + E_z^2\right) - k_0^2 \frac{\alpha_2}{2}\left(E_x^2 + E_z^2\right)^2 + C_0, \tag{22}$$

where the linear permittivity of the core $\epsilon_{l,2}$ and the nonlinear parameter $\alpha_2$ of the core appear (see Table I), and $C_0$ denotes the integration constant.

In problems with a semi-infinite nonlinear medium, the magnetic field $H_y$ and its $x$ derivative vanish when $x \to \pm\infty$. In such cases, these boundary conditions allow us to set the integration constant $C_0$ in Eq. (22) to zero [16]. Here, we deal with a problem in which the nonlinear medium is sandwiched between two linear (metal) layers, and therefore the nonlinear medium has a finite size. In this case, the integration constant cannot be set automatically to zero.

The comparisons of the right-hand side of Eq. (22) with the square of the right-hand side of Eq. (21a) gives

$$\left(\epsilon_2^2/\beta^2 - 2\epsilon_2\right)E_z^2 + \epsilon_{l,2}\left(E_x^2 + E_z^2\right) + \alpha_2/2\left(E_x^2 + E_z^2\right)^2 = C_0. \tag{23}$$

Equation (23) together with continuity conditions for the tangential components of the electromagnetic field will be helpful in finding the constraints reducing the parameter space where the solutions of Maxwell's equations are sought, in order to find the dispersion curves for the NSW configuration.

We warn that the quantities $A_x$, $A_z$ and $B_x$, $B_z$ defined below denote the amplitudes of the electric-field components at the outer side of core interfaces (in the metal cladding layers). On the contrary, the quantities $E_{x,0}$, $E_{z,0}$ and $E_{x,d}$, $E_{z,d}$ refer to the amplitudes of the electric fields at the inner interfaces of the core (in the nonlinear dielectric). We use the continuity conditions for the tangential components of the electromagnetic field in order to relate the values of the electric-field components $E_x$ and $E_z$ at the nonlinear interfaces $x = 0^+$ and $x = d^-$ to the values of the total electric-field amplitude, defined as

$$E_p \equiv \sqrt{E_{x,p}^2 + E_{z,p}^2}, \tag{24}$$

where the additional subscript $p \in \{0,d\}$ denotes the $x$ coordinate at which the quantity is calculated. The field distributions for the electric-field components in the semi-infinite linear metal regions are found by solving linear wave equations for these components. The components of the electric field in the cladding metal layers are given by the following.

(1) In the left metal region ($x < 0$—layer 1 in Fig. 1):

$$E_{x,1} = A_x e^{k_0 q_1 x}, \quad E_{z,1} = A_z e^{k_0 q_1 x}. \tag{25}$$

(2) In the right metal region ($x > d$—layer 3 in Fig. 1):

$$E_{x,3} = B_x e^{-k_0 q_3 (x-d)}, \quad E_{z,3} = B_z e^{-k_0 q_3 (x-d)}. \tag{26}$$

Only one exponential term is present in each of the expressions so that the electric field decays exponentially for $x \to \pm\infty$. The pairs of parameters $A_x$, $A_z$ and $B_x$, $B_z$ are not independent and the relationship between them can be found using Eq. (21b) for linear and uniform layers.

Using the continuity conditions for the tangential field components ($H_y$ and $E_z$) at both interfaces ($x = 0$ and $x = d$) allows us to find four relations between the electric-field amplitudes at the outer interfaces ($A_x$, $A_z$, $B_x$, $B_z$) and the inner left ($E_{x,0}$, $E_{z,0}$) and the inner right ($E_{x,0}$, $E_{z,0}$) interfaces:

$$A_z = E_{z,0}, \tag{27a}$$

$$B_z = E_{z,d}, \tag{27b}$$

$$A_x = \epsilon_{2,0} E_{x,0}/\epsilon_1, \tag{27c}$$

$$B_x = \epsilon_{2,d} E_{x,d}/\epsilon_3, \tag{27d}$$

where $\epsilon_{2,0}$ denotes the value of the nonlinear permittivity at the left interface of the core and is equal to $\epsilon_2|_{x=0^+} = \epsilon_{l,2} + \alpha_2 E_0^2$, and $\epsilon_{2,d}$ denotes the value of the nonlinear permittivity at the right interface of the core and is equal to $\epsilon_2|_{x=d^-} = \epsilon_{l,2} + \alpha_2 E_d^2$. The relations given by Eqs. (27) together with Eqs. (2b) and (2c) in the linear layers allow us to express the electric-field components at the left interface $x = 0^+$ ($E_{x,0}$, $E_{z,0}$) as a function of the total electric-field amplitude at this interface $E_0$:

$$E_{x,0}^2 = (\epsilon_1 \beta E_0)^2/[(\epsilon_{2,0} q_1)^2 + (\epsilon_1 \beta)^2], \tag{28a}$$

$$E_{z,0}^2 = (\epsilon_{2,0} q_1 E_0)^2/[(\epsilon_{2,0} q_1)^2 + (\epsilon_1 \beta)^2]. \tag{28b}$$

Similarly, we can express the electric-field components at the right interface $x = d^-$ ($E_{x,d}$, $E_{z,d}$) as a function of a total electric-field amplitude at this interface $E_d$:

$$E_{x,d}^2 = (\epsilon_3 \beta E_d)^2/[(\epsilon_{2,d} q_3)^2 + (\epsilon_3 \beta)^2], \tag{29a}$$

$$E_{z,d}^2 = (\epsilon_{2,d} q_3 E_d)^2/[(\epsilon_{2,d} q_3)^2 + (\epsilon_3 \beta)^2]. \tag{29b}$$

Equation (23) can now be rewritten on each interface in such a way that it depends only on the total electric-field amplitude at this interface (as a parameter), the effective index $\beta$ as an unknown, and the optogeometric material parameters which are known and fixed for a given NSW. Inserting Eqs. (28a) and (28b) into Eq. (23) taken at $x = 0^+$, we obtain the nonlinear dispersion relation at the left interface ($x = 0$):

$$\frac{\left[\left(\frac{\epsilon_{2,0}}{\beta}\right)^2 - 2\epsilon_{2,0}\right](\epsilon_1\beta)^2}{(\epsilon_{2,0} q_1)^2 + (\epsilon_1 \beta)^2} + \epsilon_{l,2} + \frac{\alpha_2}{2} E_0^2 = \frac{C_0}{E_0^2}. \tag{30}$$

Inserting Eqs. (29a) and (29b) into Eq. (23) taken at $x = d^-$, we obtain the dispersion relation at the right interface ($x = d$). It is identical to Eq. (30) after the substitutions: $\epsilon_{2,0}$ by $\epsilon_{2,d}$, $\epsilon_1$ by $\epsilon_3$, and $E_0$ by $E_d$.

Comparing the dispersion relation for the single interface at $x = 0$ [Eq. (30)] with the one obtained at $x = d$, we eliminate the integration constant $C_0$ and obtain the final equation of the IM:

$$\frac{\left[\left(\frac{\epsilon_{2,0}}{\beta}\right)^2 - 2\epsilon_{2,0}\right]\frac{(\epsilon_1\beta)^2}{(\epsilon_{2,0}q_1)^2+(\epsilon_1\beta)^2} + \epsilon_{l,2} + \frac{\alpha_2}{2}E_0^2}{\left[\left(\frac{\epsilon_{2,d}}{\beta}\right)^2 - 2\epsilon_{2,d}\right]\frac{(\epsilon_3\beta)^2}{(\epsilon_{2,d}q_3)^2+(\epsilon_3\beta)^2} + \epsilon_{l,2} + \frac{\alpha_2}{2}E_d^2} = \frac{E_d^2}{E_0^2}. \quad (31)$$

Equation (31) represents the constraint that will be used in the numerical algorithm computing the dispersion curves presented in Sec. III C 2, in order to reduce the dimension of the parameter space where the solutions of Maxwell's equations in NSW structures are sought.

It is worth noticing that, in Eq. (31), neither the wavelength of light $\lambda$ nor the width of the waveguide core $d$ appear. This means that the condition given by Eq. (31) is identical, regardless of the values of $\lambda$ and $d$. This condition depends only on the material parameters ($\epsilon_1$, $\epsilon_{l,2}$, $\alpha_2$, and $\epsilon_3$) and the field intensities at both nonlinear core interfaces ($E_0$ and $E_d$). The size of the core and the wavelength will appear in our next step—the numerical integration of Maxwell's equations leading to the field profiles in the core of the waveguide and to the dispersion curves of the NSW.

As stated before, Eq. (31) is not a dispersion relation for the slot waveguide modes but only a constraint that limits the parameter space where the solutions in the frame of the IM can be found. In order to obtain the dispersion relations in the NSW, the field profiles in the core are found by numerical integration of Maxwell's equations. Maxwell's equations are written as a set of coupled equations relating both electric-field components $E_x$ and $E_z$. These equations are derived from Eqs. (21a) and (21b):

$$\frac{dE_x}{dx} = k_0 \frac{\beta\epsilon_2 E_z - 2\alpha_2 E_z E_x^2\left(\beta - \frac{\epsilon_2}{\beta}\right)}{\epsilon_2 + 2\alpha_2 E_x^2}, \quad (32a)$$

$$\frac{dE_z}{dx} = k_0\left(\beta - \frac{\epsilon_2}{\beta}\right)E_x. \quad (32b)$$

#### 2. Numerical algorithm and nonlinear dispersion relations

In this section, we present the description of the numerical algorithm that is used to find the dispersion relation for the modes of a NSW in the frame of the IM. This algorithm uses the shooting method [45] to find solutions of Maxwell's equations in the waveguide core and finally the nonlinear dispersion relation for the NSW.

In a general case, the numerical procedure would be the following. First, for a given structure, we fix the parameters $E_0$, $E_d$, and $\beta$ and integrate Maxwell's equations [Eqs. (32)] in the waveguide core with the values $E_0$ and $\beta$ as initial parameters. The results of the integration are the field profiles $E_x(x)$ and $E_z(x)$ inside the nonlinear core and, in particular, the computed total electric field amplitude at the interface $x = d$ denoted by $E_d^{(\mathrm{num})}$. Next, we verify if the result of the numerical integration fulfills the conditions resulting from the problem formulation as follows.

(1) Is $E_d^{(\mathrm{num})}$ equal to the initially fixed value $E_d$?

(2) Does the $x$ derivative of the product of the permittivity and the transverse electric field $\epsilon_2 E_x$ at the interface $x = d^-$ have the correct sign? The condition for the correct sign reads

$$E_{x,d}\left.\frac{d(\epsilon_2 E_x)}{dx}\right|_{x=d^-} = -k_0 q_3 \epsilon_3 B_x^2, \quad (33)$$

and it is derived in Ref. [76]. The right-hand side of Eq. (33) is positive as $\epsilon_3$ of the metal is negative and all the other quantities there are positive. Therefore, the sign of the derivative $[d(\epsilon_2 E_x)/dx]|_{x=d^-}$ must be identical to the sign of $E_{x,d}$.

(3) Do the components of electric field at $x = d$ fulfill the conditions given by Eqs. (29a) and (29b)?

If these three conditions are fulfilled, then the triplet ($E_0$, $E_d$, and $\beta$) and the corresponding field profiles are accepted as a genuine solution of our problem.

In the general case described above, the parameter space where the solutions are sought is three dimensional and it is spanned by $E_0$, $E_d$, and $\beta$. In standard problems, the dimension of this parameter space can be further reduced by constraints resulting from, e.g., structure symmetry. Usually it relates the values of the electric field $E_0$ and $E_d$, leaving two independent variables $E_0$ and $\beta$. However, we remind that the choice of the independent variables is arbitrary, and it is often the computational simplicity or efficiency that determines this choice.

In our eigenvalue problem derived from Maxwell's equations for layered structures with a nonlinear guiding layer, we split the solution-search procedure into two cases, in which we will be able to simplify it and look for the solutions in only two-dimensional spaces. The reason for the split is the fact that the constraint reducing the dimension of the parameter space where the solutions are sought is different for each of the cases. The two cases allowing us to investigate our problem in an efficient way are as follows.[1]

(1) The case of symmetric ($E_{x,0} = E_{x,d}$) or antisymmetric solutions ($E_{x,0} = -E_{x,d}$) (for both symmetric and antisymmetric solutions $E_0 = E_d$) in a symmetric NSW ($\epsilon_1 = \epsilon_3$). In this case, we look for the solutions of Maxwell's equations in a two-dimensional space spanned by $E_0$ and $\beta$ for each of the cases $E_{x,0} = \pm E_{x,d}$. For $E_0 = E_d$ in symmetric structures, Eq. (31) represents an identity and it is satisfied for all values of $\beta$. Therefore, Eq. (31) will not provide any help in further reducing the parameter space where the solutions are sought.

(2) The case of either the asymmetric solutions ($E_0 \neq E_d$) in a symmetric NSW structure ($\epsilon_1 = \epsilon_3$) or any solution in an asymmetric NSW ($\epsilon_1 \neq \epsilon_3$). For these types of solutions,

[1]In the second case, we use a nonstandard approach, where the free parameters are chosen in a different way than in the traditional shooting method [45]. Nonetheless, the numerical results obtained with this approach are physically meaningful, as it can be seen from the numerical examples presented in the following article [44] (the results of our shooting method used for asymmetric structures converge, in the limiting case of a symmetric structure, to the results of a standard shooting method). The mathematical proof of the equivalence of these two approaches is beyond the scope of this work.

Eq. (31) is not an identity and results in a constraint on the three-dimensional space where the solutions are sought. Equation (31) is transformed to the form

$$p_4\beta^4 + p_2\beta^2 + p_0 = 0, \tag{34}$$

where

$$\begin{aligned} p_4 &= 2\epsilon_{2,d}\epsilon_3^2E_d^2(\epsilon_{2,0}^2+\epsilon_1^2) - 2\epsilon_{2,0}\epsilon_1^2E_0^2(\epsilon_{2,d}^2+\epsilon_3^2) \\ &\quad + f(\epsilon_{2,0}^2+\epsilon_1^2)(\epsilon_{2,d}^2+\epsilon_3^2), \qquad (35a)\\ p_2 &= \epsilon_{2,0}^2\epsilon_1^2E_0^2(\epsilon_{2,d}^2+\epsilon_3^2) - \epsilon_{2,d}^2\epsilon_3^2E_d^2(\epsilon_{2,0}^2+\epsilon_1^2) \\ &\quad + 2\epsilon_{2,0}\epsilon_{2,d}\epsilon_1\epsilon_3(\epsilon_{2,d}\epsilon_1E_0^2 - \epsilon_{2,0}\epsilon_3E_d^2) \\ &\quad - f[\epsilon_{2,0}^2\epsilon_1(\epsilon_{2,d}^2+\epsilon_3^2) + \epsilon_{2,d}^2\epsilon_3(\epsilon_{2,0}^2+\epsilon_1^2)], \qquad (35b)\\ p_0 &= \epsilon_{2,0}^2\epsilon_{2,d}^2\epsilon_1\epsilon_3(\epsilon_3E_d^2 - \epsilon_1E_0^2 + f), \qquad (35c)\\ f &= \epsilon_{l,2}(E_0^2+E_d^2) + \frac{\alpha_2}{2}(E_0^4+E_d^4). \qquad (35d) \end{aligned}$$

This shows that Eq. (31) is satisfied only by a finite set of $\beta$ values. Since we look for forward-propagating nonlinear modes and material losses are neglected, the only physically meaningful solutions of Eq. (34) are the ones where $\beta$ is real and positive. Therefore, the two possible roots are

$$\beta_\pm = \sqrt{\frac{-p_2 \pm \sqrt{p_2^2 - 4p_4p_0}}{2p_4}}. \tag{36}$$

Only the real solutions among $\beta_\pm$ are used further in the process of the resolution of the nonlinear problem.

Using Eq. (31), the three-dimensional space from the general case is now reduced to a two-dimensional space [one for each of the real effective indices given by Eq. (36)] spanned by $E_0$ and $E_d$. Therefore, instead of scanning a full three-dimensional space spanned by $E_0$ and $E_d$, and $\beta$ we need to scan only a two-dimensional space spanned by $E_0$ and $E_d$, and finally to test only $\beta$ values given by Eq. (36). In other words, for a pair ($E_0$, $E_d$) we just need to check if the field integration gives valid results [i.e., if conditions (1)–(3), page 6 in Sec. III C 2 are fulfilled] for real values among $\beta_\pm$. If all the conditions are fulfilled, then the triplet ($E_0$, $E_d$, and $\beta$) and the corresponding field profiles are accepted as a genuine solution of our problem.

Note that for the case (2) associated with asymmetric solutions, we reduce the phase space of possible solutions in terms of the effective index $\beta$. Another option would be to try to solve Eq. (31) with respect to $E_d$. However, this way of proceeding would be more cumbersome for this case of asymmetric solutions in our problem. It turns out that Eq. (31) can be written as a polynomial of $E_d$ in a form $E_d^8 + r_6E_d^6 + r_4E_d^4 + r_0 = 0$. This equation can be reduced to a fourth-order polynomial in $E_d^2$, for which finding solutions is more difficult than in the case of Eq. (34) that is reducible to a second-order polynomial equation in $\beta^2$. The block scheme representing the full numerical procedure to find the dispersion relation is given in Ref. [76].

## IV. CONCLUSIONS

We have presented two complementary models based on Maxwell's equations to study the properties of the stationary TM solutions in planar nonlinear structures made of a focusing Kerr nonlinear dielectric core surrounded by semi-infinite metal regions. The first model uses a simplified treatment of the nonlinearity that takes into account only the transverse component of the electric field in the nonlinear term and assumes that the nonlinear refractive index change is small compared to the linear refractive index. It provides an analytical description of both the field profiles, in the whole waveguide using Jacobi elliptic special functions, and the nonlinear dispersion relations. These features allow one to study rapidly and accurately the properties of the NSW structures as a function of their opto-geometric parameters. The second model takes into account the full dependency of the Kerr nonlinear term on all electric-field components and no assumption is required on the amplitude of the nonlinear term. It allows us both to determine the domain of validity of the first model and to investigate with accuracy the effects of high nonlinearities. These two models prove their usefulness in the next article (Ref. [44]) where we provide a complete and accurate study of nonlinear slot waveguides. It is worth mentioning that these models can be extended to more complicated geometries, refractive index forms, and/or nonlinear terms.

## ACKNOWLEDGMENTS

This work was supported by the European Commission through the Erasmus Mundus Joint Doctorate Programme Europhotonics (Grant No. 159224-1-2009-1-FR-ERA MUNDUS-EMJD). G.R. would like to thank the Scilab consortium and the Free Software Foundation.

## APPENDIX: LIMITING CASES FOR TWO-LAYER STRUCTURES

In this section we will derive the expressions for the dispersion relations in the limiting case of the single interface between a metal and a nonlinear dielectric. This will prove that our models reproduce already known results for simpler structures. These limiting case dispersion relations will also provide approximated analytical expressions for the propagation constant of highly asymmetric modes of NSW that resemble nonlinear plasmons on a single interface as shown in the following article [44].

### 1. Jacobi elliptic function based model

In Sec. III B, we have stated that in the case of a semi-infinite nonlinear medium (a single interface between a metal and a nonlinear dielectric) the integration constant in Eq. (7) should be set to zero as both the magnetic field $H_y$ and its derivative tend to zero at infinity. One way to find the dispersion relation for nonlinear waves propagating along a single interface is to use Eq. (9). Setting $c_0 = 0$ in this equation we obtain an analytical formula for the effective indices:

$$(\epsilon_{l,2}/\epsilon_1)^2q_1^2 - q_2^2 + \frac{a_2}{2}H_0^2 = 0. \tag{A1}$$

Using the definitions of $q_k$ and $a_2$ [see Table I, Eq. (6), and the text after Eqs. (8)] in Eq. (A1), we find the analytical expression for the effective index of a nonlinear wave at a single interface between a metal and a nonlinear dielectric in an explicit form:

$$\beta = \sqrt{\frac{\epsilon_1 \epsilon_{l,2}(\epsilon_{l,2} - \epsilon_1)}{\epsilon_{l,2}^2 - \epsilon_1^2 + \frac{n_2^{(2)}\epsilon_1^2 H_0^2}{2\epsilon_0 c \epsilon_{l,2}}}}. \tag{A2}$$

Another way to find the dispersion relation for nonlinear waves propagating along a single interface is to set $c_0 = 0$ at the later stage of the JEM derivation, namely in Eqs. (16) or (19) and in the definitions of the related parameters [Eqs. (13) or (18), respectively]. In both cases, this procedure yields [76] (using the expressions for the limiting values of Jacobi elliptic functions in the case of the parameter $m = 1$ provided in Ref. [24])

$$\tanh\left[k_0 q_2 (d - x_0)\right] = \frac{\epsilon_{l,2} q_3}{\epsilon_3 q_2}. \tag{A3}$$

Equation (A3) describes the nonlinear dispersion relation for plasmon solitons on a single interface (at $x = d$) between a metal and a nonlinear dielectric. Equation (A3) is equivalent to Eq. (42) from Ref. [16], which gives the dispersion relation for a single metal-nonlinear dielectric interface obtained using the field based model developed in Ref. [16], taking into account that (i) in the frame of the JEM we used the assumption that $\epsilon_2 = \epsilon_{l,2}$ in the continuity conditions used to derive the nonlinear dispersion relations (see Sec. III B) and (ii) in Ref. [16] the interface is located at $x = 0$.

Equations (A2) and (A3) give also approximated expressions for the effective indices of highly asymmetric solutions in NSWs, as it will be proven by the numerical results presented in Ref. [44]. Highly asymmetric solutions are strongly localized on one of the interfaces and therefore the problem can be simplified to a single-interface problem. A comparison of the approximated solution given by Eqs. (A2) and (A3) with the exact solutions of the JEM will be given in Sec. III B of Ref. [44].

It is worth noting that using Eq. (A2) in the linear case ($H_0 \to 0$ or $n_2^{(2)} \to 0$), we recover the dispersion relation for a linear surface plasmon propagating along a single interface [see Eq. (2.14) in Ref. [79]]:

$$\beta = \sqrt{\epsilon_1 \epsilon_{l,2}/(\epsilon_1 + \epsilon_{l,2})}. \tag{A4}$$

### 2. Interface model

Equation (30) and the corresponding one obtained at $x = d$, when considered separately, give the dispersion relation for a single interface between a metal and a nonlinear dielectric. In this case, the nonlinear medium is semi-infinite which means that $C_0$ must be set to zero (see Sec. III C 1). Setting $C_0 = 0$ in Eq. (30) yields

$$\frac{\left[\left(\frac{\epsilon_{2,0}}{\beta}\right)^2 - 2\epsilon_{2,0}\right](\epsilon_1\beta)^2}{(\epsilon_{2,0}q_1)^2 + (\epsilon_1\beta)^2} + \epsilon_{l,2} + \frac{\alpha_2}{2}E_0^2 = 0. \tag{A5}$$

This equation can be solved analytically for $\beta$. The solution depends on the parameters of the structure ($\epsilon_1, \epsilon_{l,2}, \alpha_2, \epsilon_3$) and on the electric-field amplitude at the interface $E_0$. It is given by

$$\beta = \sqrt{\frac{\epsilon_1 \epsilon_{2,0}^2\left(\epsilon_{l,2} - \epsilon_1 + \frac{\alpha_2}{2}E_0^2\right)}{\left(\epsilon_{2,0}^2 + \epsilon_1^2\right)\left(\epsilon_{l,2} + \frac{\alpha_2}{2}E_0^2\right) - 2\epsilon_1^2\epsilon_{2,0}}}. \tag{A6}$$

Only the positive root is considered because we are interested here in forward-propagating waves only. Equation (A6) can be compared to Eq. (11) in Ref. [74] and to Eq. (14) in Ref. [10] derived for the case of a single metal-nonlinear dielectric interface.

The solution for a single-interface problem provides a good approximation (in terms of effective index $\beta$ and field profiles) for first-order highly asymmetric modes in the NSWs whose field profiles are mostly localized on one interface of the core (see also the discussion in Sec. A 1). These solutions are invariant with respect to the waveguide width as they interact strongly only with one of the core interfaces. More comments and illustrations of this property will be presented in Sec. III B in Ref. [44], where we discuss the results for the symmetric NSWs. In the linear limit $\alpha_2 E_0^2 \to 0$, Eq. (A6) transforms to Eq. (A4), as expected.


[1] V. M. Agranovich, V. S. Babichenko, and V. Y. Chernyak, JETP Lett. **32**, 512 (1980).
[2] A. A. Maradudin, in *Optical and Acoustics Waves in Solids — Modern Topics*, edited by M. Borissov (World Scientific, Singapore, 1983), pp. 72–142.
[3] G. I. Stegeman and C. T. Seaton, Opt. Lett. **9**, 235 (1984).
[4] G. I. Stegeman, J. D. Valera, C. T. Seaton, J. Sipe, and A. A. Maradudin, Solid State Commun. **52**, 293 (1984).
[5] G. I. Stegeman, C. T. Seaton, J. Ariyasu, R. F. Wallis, and A. A. Maradudin, J. Appl. Phys. **58**, 2453 (1985).
[6] J. Ariyasu, C. T. Seaton, G. I. Stegeman, A. A. Maradudin, and R. F. Wallis, J. Appl. Phys. **58**, 2460 (1985).
[7] D. Mihalache, D. Mazilu, and F. Lederer, Opt. Commun. **59**, 391 (1986).
[8] A. D. Boardman, A. A. Maradudin, G. I. Stegeman, T. Twardowski, and E. M. Wright, Phys. Rev. A **35**, 1159 (1987).
[9] D. Mihalache, G. I. Stegeman, C. T. Seaton, E. M. Wright, R. Zanoni, A. D. Boardman, and T. Twardowski, Opt. Lett. **12**, 187 (1987).
[10] H. Yin, C. Xu, and P. M. Hui, Appl. Phys. Lett. **94**, 221102 (2009).
[11] K. Y. Bliokh, Y. P. Bliokh, and A. Ferrando, Phys. Rev. A **79**, 041803 (2009).
[12] W. Walasik, V. Nazabal, M. Chauvet, Y. Kartashov, and G. Renversez, Opt. Lett. **37**, 4579 (2012).
[13] C.-C. Huang, Opt. Express **20**, 13014 (2012).
[14] C. Milián, D. E. Ceballos-Herrera, D. V. Skryabin, and A. Ferrando, Opt. Lett. **37**, 4221 (2012).

[15] A. Ferrando, C. Milián, and D. V. Skryabin, J. Opt. Soc. Am. B **30**, 2507 (2013).
[16] W. Walasik, G. Renversez, and Y. V. Kartashov, Phys. Rev. A **89**, 023816 (2014).
[17] V. K. Fedyanin and D. Mihalache, Z. Phys. B **47**, 167 (1982).
[18] W. R. Holland, J. Opt. Soc. Am. B **3**, 1529 (1986).
[19] A. D. Boardman and P. Egan, IEEE J. Quantum Electron. **22**, 319 (1986).
[20] W. Chen and A. A. Maradudin, J. Opt. Soc. Am. B **5**, 529 (1988).
[21] U. Langbein, F. Lederer, and H.-E. Ponath, Opt. Commun. **46**, 167 (1983).
[22] N. N. Akhmediev, R. F. Nabiev, and Y. M. Popov, Opt. Commun. **72**, 190 (1989).
[23] D. Mihalache, D.-K. Baboiu, M. Ciumac, and D. Mazilu, Opt. Quantum Electron. **26**, S311 (1994).
[24] *Handbook of Mathematical Functions With Formulas, Graphs, and Mathematical Tables*, edited by M. Abramowitz and I. A. Stegun (Dover, New York, 1964).
[25] U. Langbein, F. Lederer, and H.-E. Ponath, Opt. Commun. **53**, 417 (1985).
[26] R. A. Sammut and C. Pask, J. Opt. Soc. Am. B **8**, 395 (1991).
[27] K. S. Chiang and R. A. Sammut, J. Opt. Soc. Am. B **10**, 704 (1993).
[28] Q. Y. Li, C. Pask, and R. A. Sammut, Opt. Lett. **16**, 1083 (1991).
[29] R. A. Sammut, C. Pask, and Q. Y. Li, J. Opt. Soc. Am. B **10**, 485 (1993).
[30] K. S. Chiang and R. A. Sammut, Opt. Commun. **109**, 59 (1994).
[31] A. D. Capobianco, B. Constantini, C. D. Angelis, G. F. Nalesso, and C. G. Someda, IEEE J. Quantum Electron. **31**, 512 (1995).
[32] N. A. Stathopoulos and J. D. Kanellopoulos, J. Opt. Soc. Am. B **14**, 1219 (1997).
[33] E. Feigenbaum and M. Orenstein, Opt. Lett. **32**, 674 (2007).
[34] A. R. Davoyan, I. V. Shadrivov, and Y. S. Kivshar, Opt. Express **16**, 21209 (2008).
[35] I. D. Rukhlenko, A. Pannipipitiya, and M. Premaratne, Opt. Lett. **36**, 3374 (2011).
[36] I. D. Rukhlenko, A. Pannipitiya, M. Premaratne, and G. P. Agrawal, Phys. Rev. B **84**, 113409 (2011).
[37] W. Walasik, A. Rodriguez, and G. Renversez, Plasmonics **10**, 33 (2015).
[38] A. R. Davoyan, I. V. Shadrivov, and Y. S. Kivshar, Opt. Express **17**, 20063 (2009).
[39] J. R. Salgueiro and Y. S. Kivshar, Appl. Phys. Lett. **97**, 081106 (2010).
[40] A. R. Davoyan, Phys. Lett. A **375**, 1615 (2011).
[41] N. Nozhat and N. Granpayeh, Opt. Commun. **285**, 1555 (2012).
[42] D. A. Smirnova, A. V. Gorbach, I. V. Iorsh, I. V. Shadrivov, and Y. S. Kivshar, Phys. Rev. B **88**, 045443 (2013).
[43] A. R. Davoyan, I. V. Shadrivov, A. A. Zharov, D. K. Gramotnev, and Y. S. Kivshar, Phys. Rev. Lett. **105**, 116804 (2010).
[44] W. Walasik, G. Renversez, and F. Ye, following paper, Phys. Rev. A **93**, 013826 (2016).
[45] W. H. Press, S. A. Teukolsky, W. T. Vetterling, and B. P. Flannery, *Numerical Recipes, The Art of Scientific Computing*, 3rd ed. (Cambridge University Press, Cambridge, UK, 2007).
[46] J. D. Jackson, *Classical Electrodynamics*, 3rd ed. (Wiley, New York, 1999).
[47] W. J. Tomlinson, Opt. Lett. **5**, 323 (1980).
[48] A. A. Maradudin, Z. Phys. B **41**, 341 (1981).
[49] K. M. Leung, Phys. Rev. A **31**, 1189 (1985).
[50] F. Lederer, U. Langbein, and H.-E. Ponath, Appl. Phys. B **31**, 69 (1983).
[51] G. J. Robbins, Opt. Commun. **47**, 309 (1983).
[52] G. I. Stegeman, C. T. Seaton, J. Chilwell, and S. D. Smith, Appl. Phys. Lett. **44**, 830 (1984).
[53] F. Lederer, U. Langbein, and H.-E. Ponath, Appl. Phys. B **31**, 187 (1983).
[54] D. Mihalache and D. Mazilu, Appl. Phys. B **37**, 107 (1985).
[55] C. T. Seaton, J. D. Valera, B. Svenson, and G. I. Stegeman, Opt. Lett. **10**, 149 (1985).
[56] C. T. Seaton, J. D. Valera, R. L. Shoemaker, and G. I. Stegeman, Appl. Phys. Lett. **45**, 1162 (1984).
[57] U. Langbein, F. Lederer, H.-E. Ponath, and U. Trutschel, Appl. Phys. B **36**, 187 (1985).
[58] U. Langbein, F. Lederer, H.-E. Ponath, and U. Trutschel, Appl. Phys. B **38**, 263 (1985).
[59] N. N. Akhmediev, Sov. Phys. JETP **56**, 299 (1982).
[60] J. V. Moloney, J. Ariyasu, C. T. Seaton, and G. I. Stegeman, Appl. Phys. Lett. **48**, 826 (1986).
[61] N. N. Akhmediev, R. F. Nabiev, and Y. M. Popov, Opt. Commun. **69**, 247 (1989).
[62] R. W. Micallef, Y. S. Kivshar, J. D. Love, D. Burak, and R. Binder, Opt. Quantum Electron. **30**, 751 (1998).
[63] R. A. Sammut, Q. Y. Li, and C. Pask, J. Opt. Soc. Am. B **9**, 884 (1992).
[64] S. Chelkowski and J. Chrostowski, Appl. Opt. **26**, 3681 (1987).
[65] J. P. Torres and L. Torner, J. Opt. Soc. Am. B **11**, 45 (1994).
[66] L. Leine, C. Wächter, and F. Lederer, J. Opt. Soc. Am. B **5**, 547 (1988).
[67] D. Mihalache, D.-K. Baboiu, and D. Mazilu, Opt. Commun. **110**, 67 (1994).
[68] D. Mihalache, D.-M. Baboiu, D. Mazilu, L. Torner, and J. P. Torres, J. Opt. Soc. Am. B **11**, 1244 (1994).
[69] D. Mihalache, M. Bertolotti, and C. Sibilia, in *Progress in Optics*, edited by E. Wolf (Elsevier, Amsterdam, 1989), Vol. XXVII, pp. 229–313.
[70] M. Fontaine, Appl. Opt. **29**, 3891 (1990).
[71] A. R. Davoyan, I. V. Shadrivov, and Y. S. Kivshar, Opt. Express **17**, 21732 (2009).
[72] A. Degiron and D. R. Smith, Phys. Rev. A **82**, 033812 (2010).
[73] C.-C. Huang, Opt. Express **20**, 18665 (2012).
[74] J.-H. Huang, R. Chang, P.-T. Leung, and D. P. Tsai, Opt. Commun. **282**, 1412 (2009).
[75] A. Ciattoni, B. Crosignani, P. D. Porto, and A. Yariv, J. Opt. Soc. Am. B **22**, 1384 (2005).
[76] W. Walasik, Ph.D. thesis, Aix–Marseille Université, 2014, https://tel.archives-ouvertes.fr/tel-01080690
[77] R. W. Boyd, *Nonlinear Optics* (Academic, New York, 2007).
[78] N. N. Akhmediev, Sov. Phys. JETP **57**, 1111 (1983).
[79] S. A. Maier, *Plasmonics: Fundamentals and Applications* (Springer, Berlin, 2007).